Spectral gain and noise evaluation of SOA and SOA-based switch matrix

D.D'Alessandro, G.Giuliani and S.Donati

Abstract: The spectral dependence of the gain and noise figure of a 1.55 μm semiconductor optical amplifier (SOA) in linear and saturated operation is calculated using an accurate description of the population inversion factor n_{sp} using a detailed density-matrix gain model, and taking longitudinal nonuniformity of carrier density into account by properly sectioning the device. Results show that the lowest noise figure is always attained at a wavelength longer than the gain peak, and that the −3 dB gain bandwidth increases in saturated operation. The performance of a SOA-based 4×4 InP switch matrix is analysed. When the matrix is in the 'on' state, it is equivalent to a cascade of three SOAs, which are analysed using longitudinal sectioning of each device, and by taking into account the amplified spontaneous emission (ASE) propagating forward and backward within the matrix. The influence of input/output passive splitter loss on the spectral noise figure of the matrix is also assessed.

1 Introduction

Semiconductor optical amplifiers (SOAs) have been successfully demonstrated as the building blocks of all-optical cross-phase and cross-gain wavelength converters and of switch matrices [1]. These devices are likely to be used in optical cross-connect (OXC) nodes operating in wavelength division multiplexing (WDM). In these applications, optical signals span a wide range of wavelengths and power levels, and accordingly, spectral gain and noise should be evaluated in both linear and saturated regimes.

The SOA spectral noise figure (NF) deserves a detailed study, because the inversion factor $n_{sp}(\lambda)$ is not so directly related to the gain $G(\lambda)$ as it is in erbium-doped fibre amplifiers (EDFAs) [2, 3]. The population inversion factor for an optical amplifier is defined as: $n_{sp} = \gamma/(\gamma - \zeta)$, where γ and ζ are, respectively, the probability of photon stimulated emission and absorption [2]. When dealing with SOAs, some authors [4] use a linear relationship between material gain g_{mat} and carrier density N (phenomenological gain model [5]), which is: $g_{mat} = a(N - N_0)$, where N_0 is the carrier density at transparency and a is a phenomenological constant. As a consequence, the inversion factor is calculated as: $n_{sp} = N/(N - N_0)$; however, N and N_0 are not truly proportional to the stimulated emission and absorption rates. A better analytical expression, neglecting waveguide loss and intraband relaxation time, is [6]

$$n_{sp} = \left[1 - \exp\left(\frac{E_{phot} - \Delta E_f}{kT}\right)\right]^{-1}$$

where E_{phot} is photon energy and ΔE_f is the difference between quasi-Fermi levels in the conduction and valence band.

In the following, we start from a detailed density-matrix gain model and compute the correct n_{sp} including intraband relaxation effects. The spectral dependence of gain and NF of a SOA is then analysed for various input powers using longitudinal sectioning of the active waveguide to take into account the effects of nonuniform longitudinal carrier density (i.e. longitudinal spatial hole-burning). For a given value of the injected current, two cases of short (400 μm) and long (600 μm) active region devices are compared, to highlight how carrier density impacts on gain and noise spectra.

A similar analysis is repeated for a 4×4 SOA-based InP switch matrix, still taking into account nonuniform carrier density within each SOA device and also accounting for the effects of forward- and backward-propagating amplified spontaneous emission (ASE) within the whole matrix. The effect of the passive waveguide loss interconnecting different SOAs is also assessed.

As a general result, it is concluded that when SOA-based devices operate in gain saturation, the gain bandwidth widens and the lowest NF is found at a wavelength notably longer than the gain peak wavelength. The results obtained can be of help in the design of complex optical systems, for which a signal may cross a large number of InP-based switch nodes.

2 SOA model and calculated results

In this section, a theoretical analysis of the SOA is carried out, giving details of the rate equation and the gain model used. Results are shown in terms of the spectral dependence of gain and NF for the device. The model explicitly considers the nonuniform longitudinal distribution of the carrier density, which arises from the strongly nonuniform optical power density of the signal and spontaneous emission along the active waveguide. A thorough analysis,

IEE Proceedings online no. 20010522

DOI: 10.1049/ip-opt:20010522

Paper first received 8th November 2000 and in revised form 22nd May 2001

The authors are with the Dipartimento di Elettronica, Università di Pavia, Via Ferrata 1, I-27100 Pavia, Italy
E-mail: giuliani@ele.unipv.it

carried out in [7], shows that a simpler model based on a uniform average carrier density can lead to inaccuracies in the calculated gain and NF values as large as 2 dB.

2.1 SOA sectioning and rate equation

The SOA is divided into M longitudinal sections (Fig. 1) and a description based on uniform averaged carrier and photon densities [8] is adopted for each section. In each section the steady-state rate equation is written as

$$\frac{I_j}{qwdL_j} = R_{\mathrm{sp},j}(N_j) + R_{\mathrm{stim,sig},j}(\mathbf{N}, S_{\mathrm{in,sig}}, \lambda_{\mathrm{sig}}) + R_{\mathrm{stim,ASE},j}(\mathbf{N}) \qquad j = 1, 2, \ldots, M \tag{1}$$

where N_j is the carrier density value of the jth section, $\mathbf{N} = (N_1, N_2, \ldots, N_M)$ is the vector of sections carrier densities, I_j is the current injected into the jth section, w is active layer width, d is active layer thickness, $L_j = L/M$ is the length of the jth section. $R_{\mathrm{sp},j}(N_j) = AN_j + BN_j{}^2 + CN_j{}^3$ is the spontaneous recombination term, while $R_{\mathrm{stim,sig},j}$ and $R_{\mathrm{stim,ASE},j}$ are the stimulated recombination rates induced into the jth section by signal and ASE photons, and they also depend on the carrier density of other sections. Signal and ASE photon densities are spatially averaged within each section and a pure travelling wave regime is assumed; hence, the stimulated recombination rates are:

$$R_{\mathrm{stim,stig},j}(\mathbf{N}, S_{\mathrm{in,sig}}, \lambda_{\mathrm{sig}}) = v_g g_{\mathrm{mat}}(N_j, \lambda_{\mathrm{sig}}) \frac{G(N_j, \lambda_{\mathrm{sig}}) - 1}{\ln G(N_j, \lambda_{\mathrm{sig}})} S_{\mathrm{in,sig},j} \tag{2a}$$

$$\begin{aligned} R_{\mathrm{stim,ASE},j}(\mathbf{N}) &= v_g \int g_{\mathrm{mat}}(N_j, \lambda)\left[\bar{\sigma}_{\mathrm{sp},j}(N_j, \lambda) + \bar{\sigma}_{\mathrm{ASE,in},j}(\mathbf{N}, \lambda)\right] d\lambda \\ &= v_g \int g_{\mathrm{mat}}(N_j, \lambda)\left[\frac{2\Gamma\beta(\lambda)\rho_{\mathrm{sp}}(N_j, \lambda)}{v_g(\Gamma g_{\mathrm{mat}}(N_j, \lambda) - \alpha)}\left(\frac{G(N_j, \lambda) - 1}{\ln G(N_j, \lambda)} - 1\right) + \frac{G(N_j, \lambda) - 1}{\ln G(N_j, \lambda)} \bar{\sigma}_{\mathrm{ASE,in},j}(\mathbf{N}, \lambda)\right] d\lambda \end{aligned} \tag{2b}$$

where g_{mat} is material gain, λ_{sig} is signal wavelength, v_g the group velocity, $S_{\mathrm{in,sig},j}$ is the input signal photon density to jth section, $G(N_j, \lambda_{\mathrm{sig}}) = \exp\{[\Gamma \cdot g_{\mathrm{mat}}(N_j, \lambda_{\mathrm{sig}}) - \alpha] \cdot L_j\}$ is the gain of the jth section, α the waveguide losses and Γ the confinement factor. The ASE term (eqn. 2b) is calculated by spectral integration of two stimulated recombination rates: one caused by the averaged spontaneous spectral photon density generated within the jth section ($\bar{\sigma}_{\mathrm{sp},j}(N_j, \lambda)$) and the other caused by the averaged ASE spectral photon density generated by all other sections that enter the jth section from both sides ($\bar{\sigma}_{\mathrm{ASE,in},j}(\mathbf{N}, \lambda)$). Calculation of the term $\bar{\sigma}_{\mathrm{sp},j}(N_j, \lambda)$ involves the spontaneous emission coupling factor $\beta = \lambda^2\Gamma/8\pi n^2 wd$ (that accounts for coupling of spontaneous photons into the guided mode) and the spectral spontaneous photon density generation rate $\rho_{\mathrm{sp}}(N, \lambda)$, which is obtained from the stimulated emission coefficient using Einstein's relation:

$$\rho_{\mathrm{sp}}(N, \lambda) = \frac{8\pi c n^2}{\lambda^4} E_{\mathrm{st}}(N, \lambda) \tag{3}$$

where n is the group index of refraction. It should be noted that the correct value of β for the SOA model is considerably larger than the one used for a laser, because one does not set any resonant condition on the spontaneous photons. Term (2b) cannot be neglected for a high gain SOA, because ASE photons cause appreciable amplifier self-saturation. Eqn. 1 represents a set of M mutually coupled nonlinear equations in the unknown $\mathbf{N}$, which is solved numerically using a least squares gradient method. The number of sections into which each SOA is divided is $M = 8$, a value that proves to give adequately accurate results [7].

2.2 Gain model

Another crucial point is the choice of the gain model adopted for the semiconductor material. In this work we consider a bulk semiconductor active material, and use a density-matrix gain model [5], taking into account light- and heavy-hole band transitions, energy gap dependence on carrier density, intraband relaxation time τ_{in} [9], and the quasi-Fermi levels are calculated according to the Joyce–Dixon approximation [5]. The model allows one to calculate the stimulated emission and the stimulated absorption coefficients $E_{\mathrm{st}}(N, \lambda)$ and $E_{\mathrm{a}}(N, \lambda)$ (from which the material gain is obtained as $g_{\mathrm{mat}} = E_{\mathrm{st}} - E_{\mathrm{a}}$) and the spontaneous generation rate $\rho_{\mathrm{sp}}(N, \lambda)$. The intraband relaxation time is accounted for by convolution in the frequency domain with a Lorentzian lineshape with FWHM $= 1/(\pi\tau_{\mathrm{in}})$.

The evaluation of $E_{\mathrm{st}}(N, \lambda)$ and $E_{\mathrm{a}}(N, \lambda)$ is important, because the complete expression for the inversion factor is [6]

$$n_{\mathrm{sp}}(N, \lambda) = \frac{\Gamma E_{\mathrm{st}}(N, \lambda)}{\Gamma[E_{\mathrm{st}}(N, \lambda) - E_{\mathrm{a}}(N, \lambda)] - \alpha} \tag{4}$$

where N is the carrier density calculated for the specified input signal wavelength and intensity. Using eqn. 4, the output ASE spectral density of an optical amplifier with uniform population inversion is obtained as: $p_{\mathrm{ASE}}(\nu) = n_{\mathrm{sp}}(G - 1)h\nu$, and the noise figure can be calculated accordingly [2]. Obviously, since in the present model we

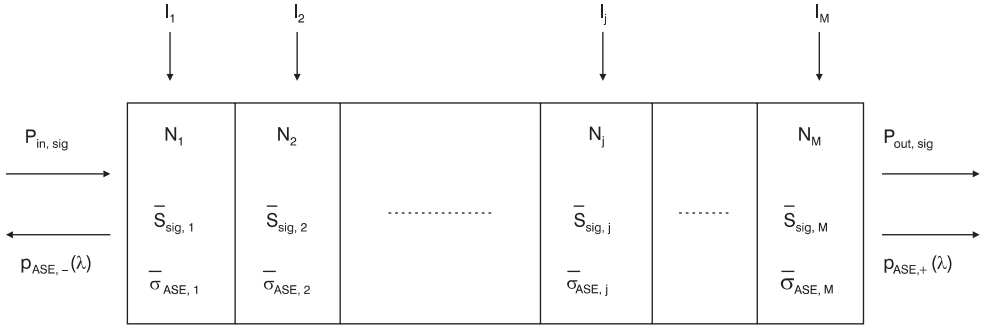

Fig. 1 *The SOA waveguide is longitudinally divided into M sections of equal length. $P_{in,sig}$ and $P_{out,sig}$ are input and output signal power, $p_{ASE,+}$ and $p_{ASE,-}$ are co- and counter-propagating ASE spectral densities. $\bar{S}_{sig,j}$ and $\bar{\sigma}_{ASE,j}$ are, respectively, the spatially averaged signal and ASE photon densities in the jth section*

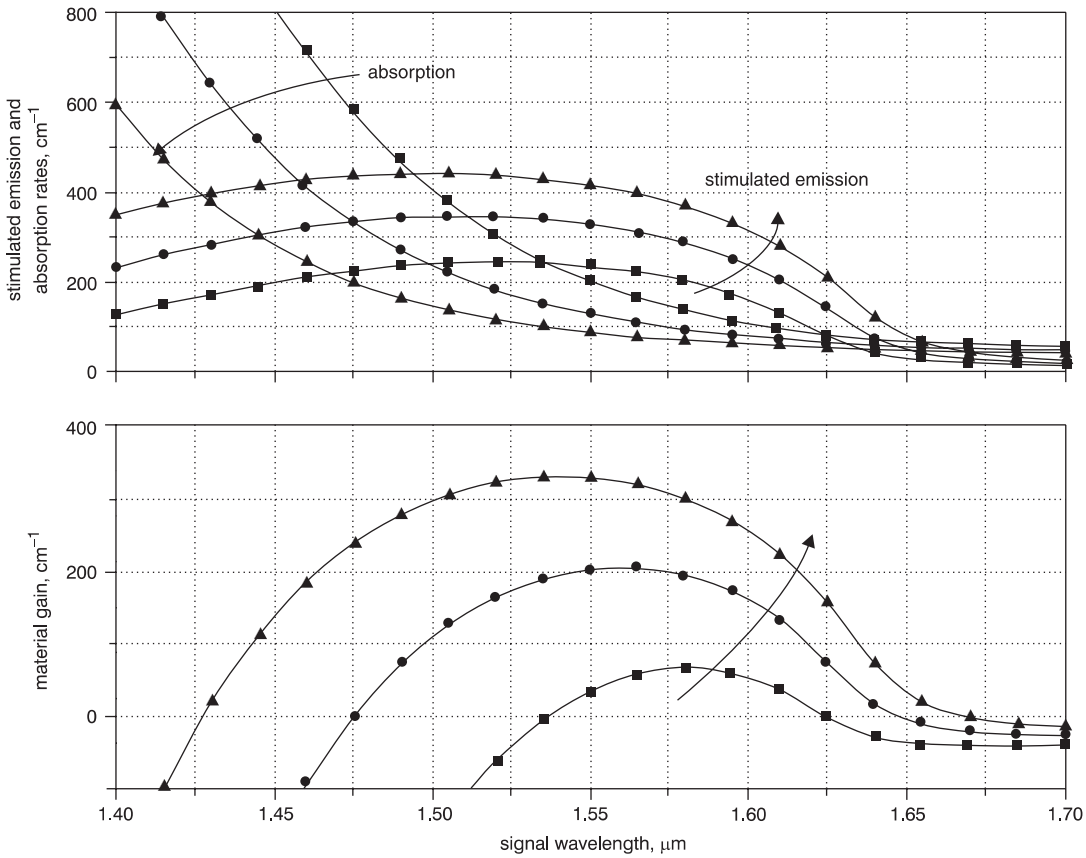

Fig. 2 *Top: Stimulated emission (E_{st}) and stimulated absorption (E_a) rate for bulk InGaAsP 1.55 μm semiconductor. Bottom: net material gain for the same carrier densities*

Injected carrier density ■ 1.5×10^{18} cm^{-3}; ● 2×10^{18} cm^{-3}; ▲ 2.5×10^{18} cm^{-3}

are explicitly considering longitudinal carrier spatial hole-burning (i.e. a SOA with nonuniform population inversion), expression (4) applies to a single section of the device. The overall device noise figure is to be found by either using the cascading formula for the NF [2] or by direct computation of the total output ASE spectral density from which the NF can be obtained by easy calculation.

In Fig. 2 the calculated stimulated emission and absorption are shown for different values of the injected carrier density; the resulting material gain is also reported. The inversion factor minimum occurs for a wavelength longer than the net-gain peak, because of the rapid increase of the absorption rate for shorter wavelengths; this effect is more pronounced for smaller carrier densities.

It should be noted that the results reported here have general validity and the proposed method can as well be applied to the case of multiquantum-well materials. Here, emphasis is placed on the need for correct material gain description to obtain reliable results for the noise of the device. Other features such as polarisation dependence are not of central importance in the present analysis, and could be taken into account by adopting a proper description for different TE/TM confinement factors and gain. In this work the performances of a bulk material 1.55 μm SOA is studied in terms of gain and NF for linear and saturated operation. For the calculation, a polarisation-insensitive SOA with a squared buried waveguide, as described in [10], is used. A summary of values for the parameters involved in the model is reported in Table 1.

2.3 Results

In Figs. 3 and 4, SOA gain and NF calculated for varying input signal power and wavelength are plotted for a short (400 μm) and a long (600 μm) device, respectively, for the same value of injected current. It should be noted that in practical devices, the calculated gain values would be obtained at higher total injected currents due to carrier leakage. In saturated operation the gain bandwidth considerably widens, and the NF is slightly reduced. The latter result is not surprising, because (as explained in detail in [7]) for moderate SOA saturation the spatial carrier density profile is modified so that the input region of the active waveguide has a higher population inversion, hence a smaller overall NF. The minimum NF for the short SOA

Table 1: Values of the parameters included in the model

α	waveguide losses	63.4 cm^{-1}	Γ	confinement factor	0.67
β	spontaneous emission factor (at 1.55 μm)	3.27×10^{-2}	τ_{in}	intraband relaxation time	10^{-13} s
A	radiative coefficient	2.8×10^{8} s^{-1}	d	active layer thickness	0.4 μm
B	nonradiative coefficient	4.26×10^{-11} cm^3 s^{-1}	w	active layer width	0.4 μm
C	Auger coefficient	6.5×10^{-29} cm^6 s^{-1}	v_g	group velocity	8.57×10^{9} cm s^{-1}

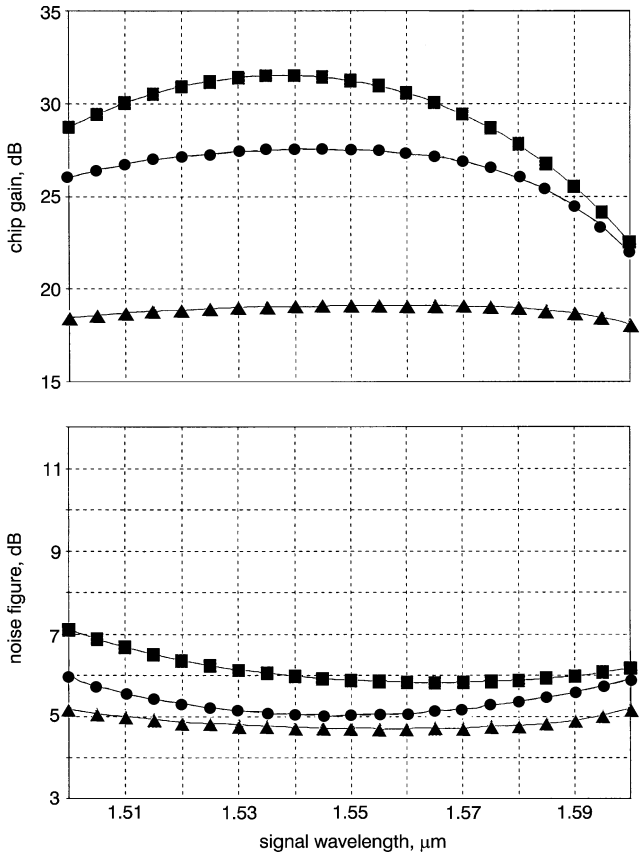

Fig. 3 *SOA gain and noise figure, calculated for varying signal wavelength for 40 mA injected current. A 1 nm output ASE filter is assumed*
Input chip facet signal power: −30 dBm (■), −20 dBm (●), −10 dBm (▲). SOA length 400 μm

is slightly below 5 dB. A performance approaching the 3 dB quantum limit cannot be obtained because of waveguide losses and material absorption. In both linear and saturated operation the NF minimum is shifted towards longer wavelengths with respect to the gain peak, in agreement with experiments [3]. This effect is more evident in saturation and for the long device, because of the occurrence of smaller carrier density values.

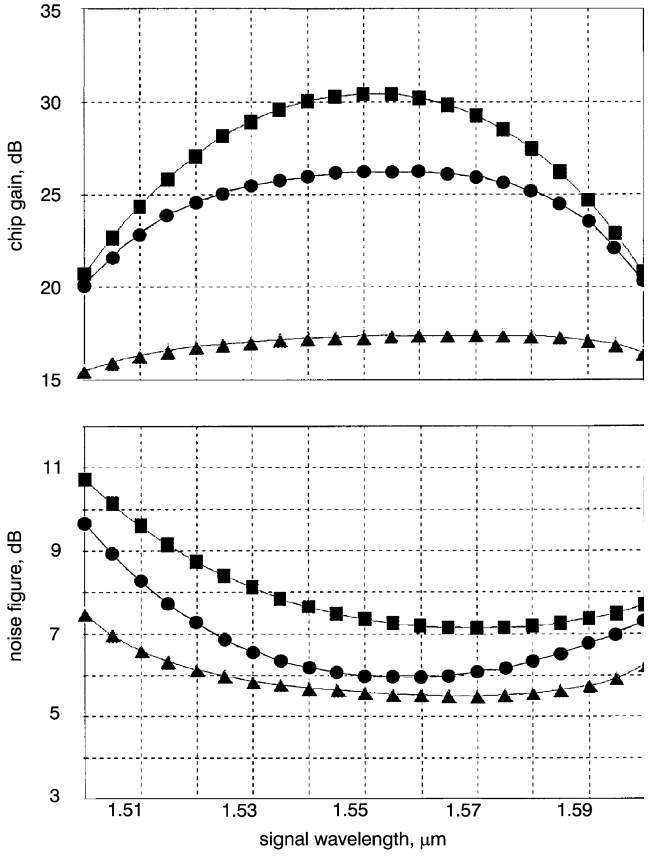

Fig. 4 *As Fig. 3 for SOA length 600 μm*

3 Application to InP 4 × 4 SOA gate switch matrix

The SOA model described above is now applied to study gain and noise characteristics of a monolithic InGaAsP-InP 4 × 4 SOA gate switch matrix [1], as an example of a practical SOA-based device. The matrix (shown in Fig. 5*a*), consists of 24 SOAs and 24 Y-junction waveguide couplers integrated on the same substrate, and it operates as a non-blocking 4 × 4 space-switch.

3.1 Switch matrix model

The matrix is analysed only for its 'on' state, because in the 'off' state noise characteristics are not relevant. In the 'on' state, the equivalent scheme of Fig. 5*b* can be applied: the matrix is described as the cascade of three SOAs with loss α_2 between each SOA accounting for Y-junction losses, and loss α_1 accounting for input/output waveguide loss and fibre coupling loss.

Each SOA is again modelled by longitudinally dividing it into $M = 8$ sections. The ASE power that propagates in the forward and backward direction within the matrix is easily taken into account, because the SOA model used also allows for the injection of an external ASE spectral density into the device. We end up with a set of $3 \times 8 = 24$ coupled rate equations (one for each SOA section) that are solved numerically to determine the carrier density within each section of the three SOAs. Thus, it is possible to compute the matrix fibre-to-fibre gain and the total output ASE spectral density, from which the NF is obtained.

3.2 Results

The analysis shows that the carrier density distribution of the three SOAs (and hence the overall switch matrix gain and noise characteristics) depends on ASE-induced device saturation for small input signal power, and on the signal intensity itself for large inputs.

In Figs. 6 and 7 gain and NF of the 4 × 4 matrix, for varying input signal power and wavelength, are reported. Each SOA is 400 μm long and is pumped at 30 mA current. Two matrix types are considered: one with Y-junction couplers exhibiting a large loss ($\alpha_2 = 18$ dB, Fig. 6), and one with low loss ($\alpha_2 = 10$ dB, Fig. 7).

- For the high loss array (Fig. 6), a 20.5 dB fibre-to-fibre unsaturated gain is attained, with a minimum NF around 12 dB (also fibre-to-fibre). In the absence of input signal, the effect of forward and backward ASE on SOAs saturation is small, because of strong ASE attenuation between each SOA due to the high loss α_2. For strong input signals the gain bandwidth widens, the NF at first decreases and then increases and its minimum is shifted to longer wavelengths.
- The low loss array (Fig. 7) exhibits almost the same gain; no relevant increase of unsaturated gain is observed, because the lower loss between SOAs causes appreciable saturation by ASE in the first SOA (input device) and in the third SOA (output device). Relevant differences between the two matrices are found in the noise figure. For input powers of −10 and 0 dBm, the NF of the high-loss matrix is respectively 2 dB and 5 dB larger.

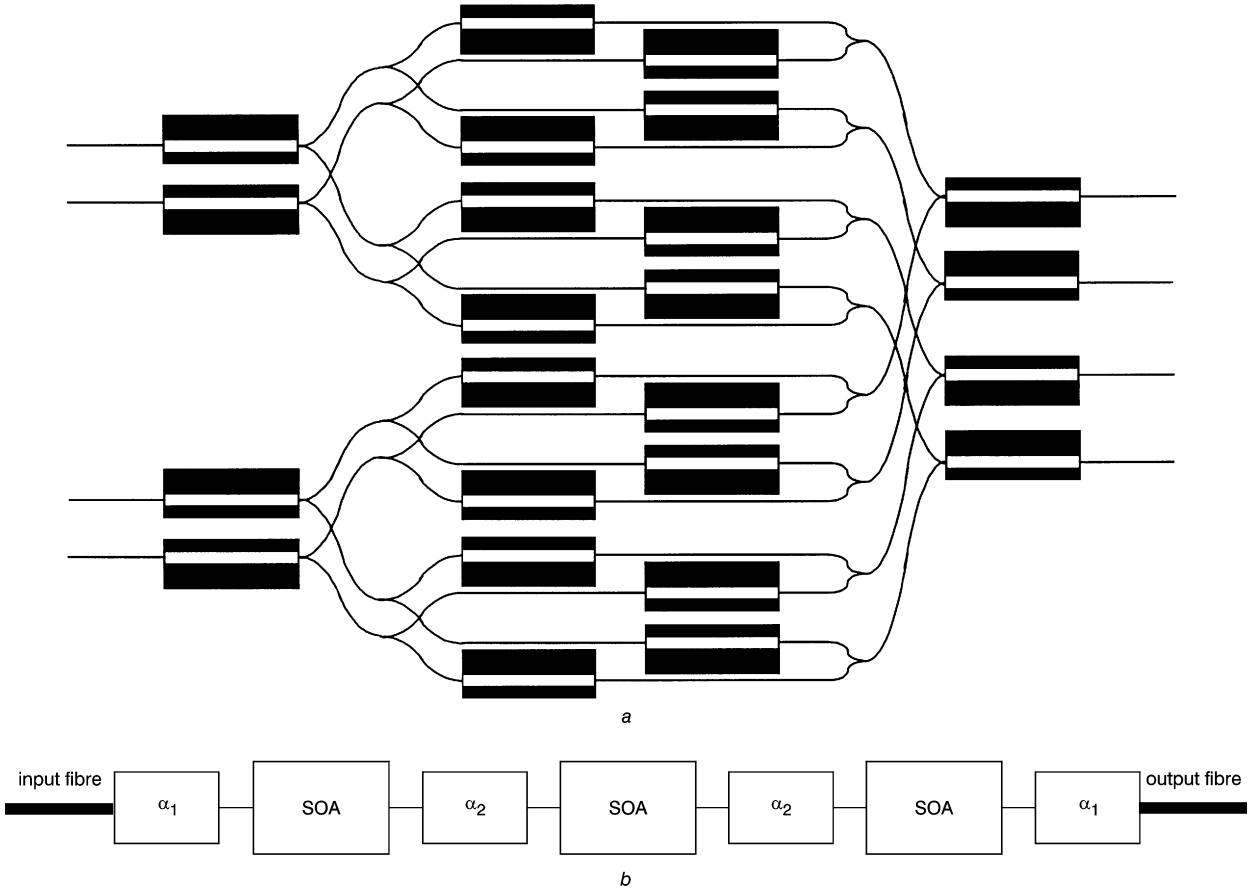

Fig. 5 *(a) Sketch of the InGaAsP-InP monolithic 4 × 4 SOA gate switch matrix described in [1], and (b) equivalent block scheme for the 'on' state*

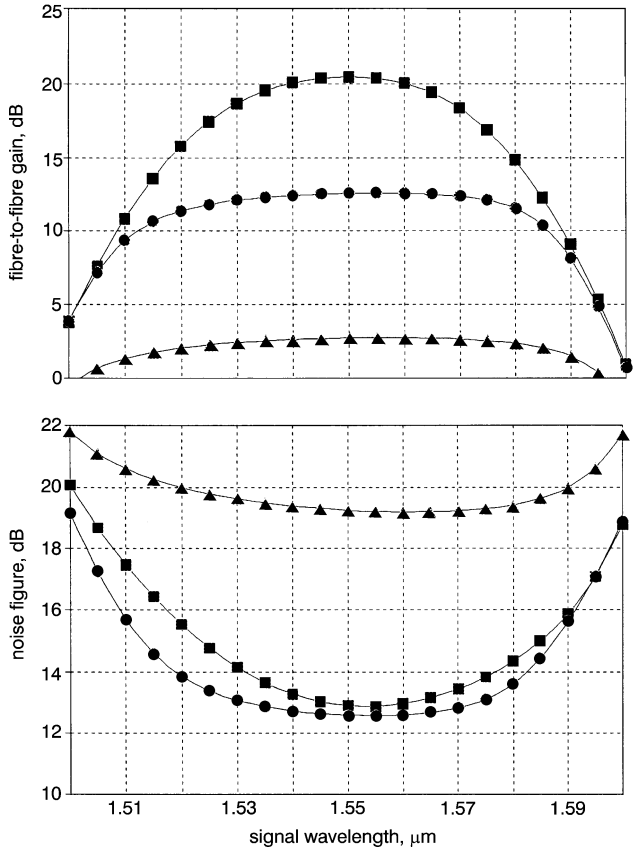

Fig. 6 *Fibre-to-fibre gain and noise figure of 4 × 4 SOA gate switch matrix in the 'on' state. A 1 nm output ASE filter is assumed*

Input fibre signal power: −20 dBm (■), −10 dBm (●), 0 dBm (▲). SOA length: $L = 400$ μm; injected current for each SOA: $I = 30$ mA; input/output loss: $\alpha_1 = 4.5$ dB. Y-junction coupler loss: α_2 18 dB

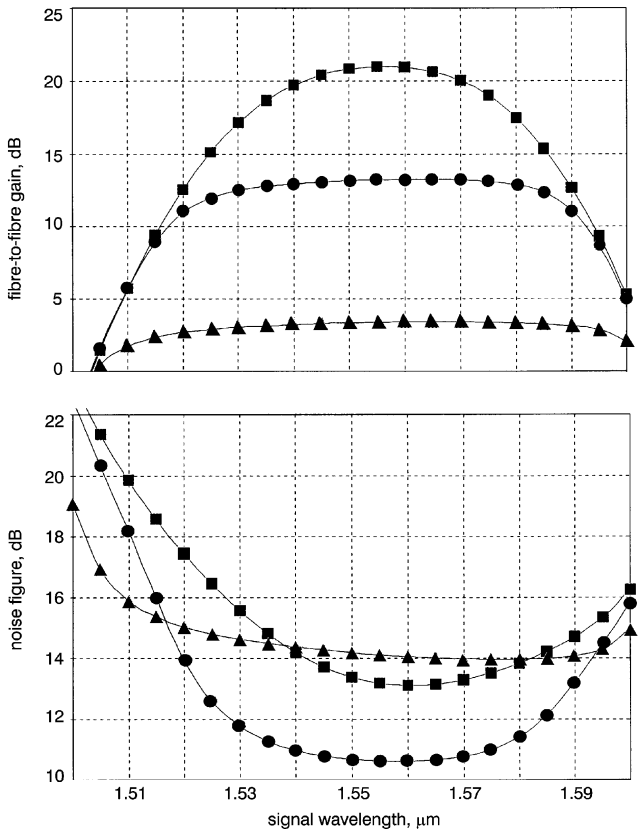

Fig. 7 *As Fig. 6 for Y-junction coupler loss α_2 10 dB*

The results obtained can be compared with those of [11], in which the SOA array is analysed with a fixed value of n_{sp} and for a single wavelength. The NF values obtained here are in general agreement with those of [11], and take advantage of the exact evaluation of n_{sp} and its spectral dependence, and of the accurate modelling of longitudinal spatial carrier hole-burning effects within each SOA.

4 Conclusion

The spectral dependence of gain and noise figure of a 1.55 μm stand-alone SOA and of a 4×4 SOA gate switch matrix has been investigated theoretically, for a wide range of input powers. To accurately calculate the n_{sp} factor, an improved model of semiconductor gain has been used together with a proper description of longitudinal carrier density hole-burning. Minimum NF is shown to be limited by waveguide loss and stimulated absorption effect. In saturated operation the gain bandwidth widens, the NF increases and the shift of NF minimum towards longer wavelengths is more pronounced. The proposed method can be useful in assessing the performance of complex optoelectronic systems including a large number of SOA-based active devices.

5 Acknowledgment

This work has been performed under a CNR-Madess II contract.

6 References

1 VAN BERLO, W., JANSON, M., LUNDGREN, L., MÀRNER, A.C., TERLECKI, J., GUSTAVSSON, M., GRANESTRAND, P., and SVENSSON, P.: 'Polarization-insensitive, monolithic 4×4 InGaAsP-InP laser amplifier gate switch matrix', *IEEE Photon. Technol. Lett.*, 1995, **7**, (11), pp. 1291–1293
2 DESURVIRE, E.: 'Erbium-doped fiber amplifiers—Principle and applications' (J. Wiley & Sons, New York, 1994)
3 HOLTMANN, C., BESSE, P.-A., BRENNER, T., and MELCHIOR, H.: 'Polarization independent bulk active region semiconductor optical amplifier for 1.3 μm wavelengths', *IEEE Photon. Technol. Lett.*, 1996, **8**, (3), pp. 343–345
4 MUKAI, T., and YAMAMOTO, Y.: 'Noise in AlGaAs semiconductor laser amplifier', *IEEE J. Quantum Electron.*, 1982, **18**, pp. 564–575
5 AGRAWAL, G.P., and DUTTA, N.K.: 'Long-wavelength semiconductor lasers' (Van Nostrand Reinhold, New York, 1986)
6 JEPSEN, K.S., MIKKELSEN, B., POVLSEN, J.H., YAMAGUCHI, M., and STUBKJAER, K.E.: 'Wavelength dependence of noise figure in InGaAs/InGaAsP multiple-quantum-well laser amplifier', *IEEE Photon. Technol. Lett.*, 1992, **4**, (6), pp. 550–553
7 GIULIANI, G., and D'ALESSANDRO, D.: 'Noise analysis of conventional and gain-clamped semiconductor optical amplifiers', *J. Lightwave Technol.*, 2000, **18**, (9), pp. 1256–1263
8 ADAMS, M.J., COLLINS, J.V., and HENNING, I.D.: 'Analysis of semiconductor laser optical amplifiers', *IEE Proc. J.*, 1985, **132**, (1), pp. 58–63
9 KAMIYA, T.: 'Radiative and non-radiative recombinations in semiconductors', *in* SUEMATSU, Y., and ADAMS, A.R. (Eds.): 'Semiconductor lasers and photonic integrated circuits' (Chapman & Hall, London, 1994)
10 KITAMURA, S., KOMATSU, K., and KITAMURA, M.: 'Very low power consumption semiconductor optical amplifier array', *IEEE Photon. Technol. Lett.*, 1995, **7**, (2), pp. 147–148
11 JEONG, G., and GOODMAN, W.: 'Gain optimization in switches based on semiconductor optical amplifiers', *J. Lightwave Technol.*, 1995, **13**, (4), pp. 598–605